Numerical modeling of diffusive heat transport across magnetic islands and highly stochastic layers

M. Hölzl, S. Günter, Q. Yu, and K. Lackner

Max-Planck-Institut für Plasmaphysik, EURATOM Association, 85748 Garching, Germany

ASDEX Upgrade

IPP

1. Introduction

In tokamak research, exact heat diffusion computations are relevant e.g. for the stability analysis of neoclassical tearing modes and the understanding of stochastic divertors. We numerically examine steady state heat transport in the presence of magnetic islands and highly stochastic layers in cylindrical geometry. Our results have been submitted to Physics of Plasmas [1].

2. Model

The steady state heat diffusion equation

$$\nabla \cdot \vec{q} = P \tag{1}$$

is solved, where

$$\vec{q} = \vec{q}_{||} + \vec{q}_{\perp} = -n\chi_{||}\nabla_{||}T - n\chi_{\perp}\nabla_{\perp}T \tag{2}$$

is the heat flux density. The temperature gradients parallel and perpendicular to the magnetic field lines are defined as $\nabla_{||}T = \hat{b}(\hat{b}\cdot\nabla T)$ resp. $\nabla_{\perp}T = (\nabla - \nabla_{||})T$, the magnetic field direction is denoted as $\hat{b} = \vec{B}/B$ and $\chi_{||}$ and $\chi_{\perp}$ are the parallel and perpendicular heat diffusion coefficients.

- Central heating $P(r) = P_0[1 - 3(r/0.2a)^2 + 2(r/0.2a)^3]$ inside $r = 0.2a$
- Boundary conditions $T(r = a) = 0$ and $\lim_{r\to 0} dT/dr = 0$
- Safety factor $q(r) = 0.9[1+(r/0.48a)^4]^{0.5}$ yielding $q(0) = 0.9$ and $q(a) = 4$
- $\chi_{||}/\chi_{\perp}$ takes values up to 10^{11} in state-of-the-art fusion experiments.

⇒ Discretization in radial and poloidal directions with a 2nd order finite difference scheme, for which numerical errors do not depend on $\chi_{||}/\chi_{\perp}$ [2, 3].

- Unsheared helical coordinate system with $\theta^* = \theta - \phi/q_c$

⇒ Rational $q_c = m_c/n_c$ allows for toroidal Fourier decomposition

⇒ Single island cases can be reduced to 2D by chosing $q_c \equiv m/n$.

⇒ For $q_c \approx m/n$, the temperature gradients along the coordinate lines are reduced which leads to smaller numerical errors:

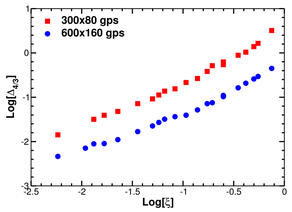

FIGURE 1: *Relative errors in $T_{i/3}$ at the resonant surface for a single 4/3 island case versus the coordinate alignment measure $\xi = |q_c^{-1} - q^{-1}|$. Approximate alignment of the coordinate system to the helicity of the perturbation significantly reduces numerical errors.*

- The sparse matrix solver package WSMP is used. [4]

3. Magnetic islands

At magnetic islands, parallel and perpendicular heat transport contribute to the radial heat diffusion. A scale island width

$$w_c = r_s(\chi_{||}/\chi_{\perp})^{-1/4}\sqrt{8/\epsilon_s s_s n} \tag{3}$$

can be defined, for which parallel and perpendicular heat transport are approximately equal. Here, r_s denotes the minor radius of the rational surface, $\epsilon_s = r_s/R_0$ the local inverse aspect ratio at r_s, and $s_s = [(r/q)\cdot\partial q/\partial r]_{r_s}$ the local magnetic shear [5].

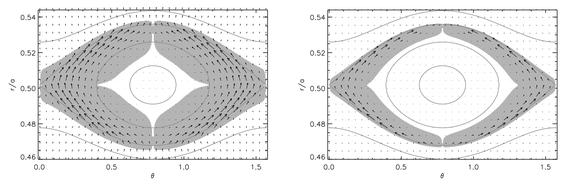

FIGURE 2: *Heat flux density around a 4/3 magnetic island with $w = 0.068a$, $\chi_{||}/\chi_{\perp} = 10^9$ resp. 10^9, $w/w_c = 3.4$ resp. 6.0. The heat conduction layer is indicated with a grey background. For clarity, the vectors in the right figure have been scaled by a factor of 0.31.*

- Inside the heat conduction layer, parallel transport around the island is possible. The temperature in the island o-point region flattens.
- Outside the heat conduction layer, the flux surfaces are closer in the o-point region than in the x-point region.

⇒ Most heat flux enters/exits the heat conduction layer in the o-point region.

⇒ Outside the heat conduction layer, parallel transport is oriented towards the o-point region for $r < r_s$ and away from the o-point for $r > r_s$.

⇒ In both regions, it has a radial component directed towards the plasma center and thus reduces the total outward radial heat flux (Fig. 3).

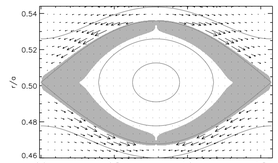

FIGURE 3: *Parallel transport outside the heat conduction layer for the same case as Fig. 2 b). It has a small radial component directed inwards.*

The effective radial heat diffusivity coefficient χ_r at the island:

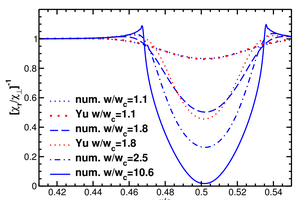

FIGURE 4: *The inverse of the radial heat diffusivity χ_r at a 4/3 magnetic island with $w = 0.068a$. For the first two cases, an analytical formula by Yu is plotted as well [6]. Although we are using it outside the range it was derived for ($w/w_c \ll 1$), the formula shows very good agreement with the numerical results for $w/w_c = 1.1$ and reasonable agreement even for $w/w_c = 1.8$.*

- χ_r is strongly increased ($\gg \chi_{\perp}$) in magnetic island regions. Outside the heat conduction layer, χ_r is slightly smaller than $\chi_{\perp}$, as the parallel heat flux has a radial component directed towards the plasma center (Fig. 3).
- The dependence of $\chi_r(r_s)$ on w/w_c is shown in Fig. 5.

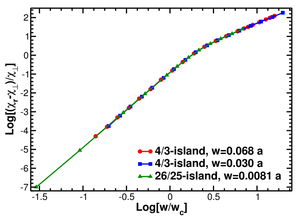

FIGURE 5: *The radial heat diffusivity χ_r at the resonant surface. Two different regimes for χ_r are observed: $\chi_r \propto [w/w_c]^4$ for $w/w_c \lesssim 1$ and $\chi_r \propto [w/w_c]^2$ for $w/w_c \gtrsim 4.5$. The agreement of the different plotted cases verifies that χ_r depends on w/w_c only as predicted by Fitzpatrick. [5]*

4. Neoclassical tearing modes (NTMs)

- Magnetic islands perturb the temperature and with it the neoclassical bootstrap current. For conventional tokamak configurations, this is a destabilizing contribution to the island drive [5, 7–9].
- Analytical examinations for the limits of small and large w/w_c have been performed by Fitzpatrick, as well as a matching between these limits [5].
- We compute the island drive in the same way, but from numerically obtained temperature perturbations.

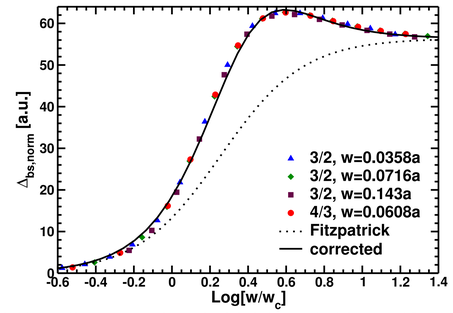

FIGURE 6: *Island drive caused by temperature perturbations. 3/2 and 4/3 island cases are plotted. Agreement with Fitzpatricks small and large island limits is found [5]. However, the widely used matching between these limits underestimates the island drive for intermediate values of w/w_c significantly. With the correction factor we propose applied, the numerical results are reproduced very well.*

⇒ Agreement with the analytical small and large island limits

⇒ For medium values of w/w_c the analytical matching underestimates the bootstrap current island drive significantly.

⇒ With the correction factor

$$\left(1 + 2.2/\left[(w/w_d)^2 + 3w_d/w\right]\right), \tag{4}$$

where $w_d \approx 1.8w_c$, the numerical results are reproduced very well.

5. Highly stochastic layers

Stochastic fields are used at the plasma edge in some tokamak experiments to acheive a more evenly distributed energy load on the walls and possibly to suppress edge localized modes (ELMs) [10, 11].

- We examine ergodic heat diffusion for an example of five overlapping magnetic islands with the helicities $q_i = 24/23, 25/24, 26/25, 27/26, 28/27$.
- Pairwise stochasticity $s_{i,j} = (w_i + w_j)/2|r_{s,i} - r_{s,j}|$ between 4 and 17.5.
- "Total stochasticity" $s = \sum_{i\neq 3} s_{i,3} = 48.5$.

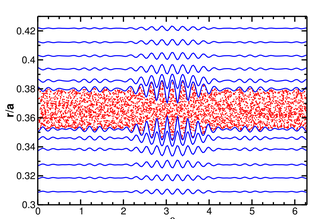

FIGURE 7: *Poincaré plot of the highly ergodic layer produced by five resonant magnetic perturbations.*

- Radial heat diffusivity χ_r is increased over the whole ergodic layer (Fig. 8).

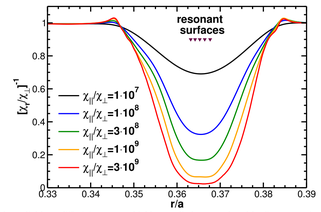

FIGURE 8: *The inverse of the radial heat diffusivity χ_r at a highly ergodic layer produced by five magnetic perturbations with very similar helicities.*

- Analytic studies of ergodic heat transport e.g. by Rechester and Rosenbluth, Stix, Kadomtsev and Pogutse, Krommes et.al., and Liewer [12–16].
- Three subregimes of the collisional regime predicted: fluid regime, Kadomtsev-Pogutse regime, and Rechester-Rosenbluth regime.
- Fluid regime recently corrected by Yu by a factor of 1/2 for our case [6].

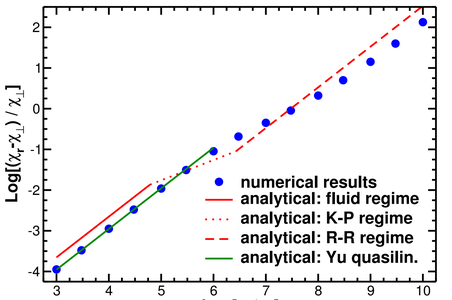

FIGURE 9: *$\kappa = (\chi_r - \chi_\perp)/\chi_\perp$ at the center of the highly ergodic layer. Qualitative agreement between the analytically predicted and the numerically observed κ is found. However, the ranges of validity of the regimes and the absolute values do not coincide. Very good quantitative agreement is observed, when the fluid regime formula is corrected according to Yu [6].*

In the limits of small and large $\chi_{||}/\chi_{\perp}$, the analytically predicted proportionalities are observed. There is also a regime with a reduced slope in the log-log plot similar to the Kadomtsev-Pogutse regime.

- Qualitative agreement with the three predicted regimes.
- Ranges of validity and absolute values do not coincide.
- Very good agreement with the corrected fluid regime results by Yu.
- Discrepancies in the Rechester-Rosenbluth regime may be due to a non-exponential contribution to the field line diffusion (Rover, Ref. [17]).

References

[1] M. Hölzl, S. Günter, Q. Yu, and K. Lackner. Phys. Plasmas (submitted).
[2] S. Günter, Q. Yu, J. Krüger, and K. Lackner. J. Comput. Phys. **209**, 354 (2005).
[3] S. Günter, K. Lackner, and C. Tichmann. J. Comput. Phys. (2007). (submitted).
[4] A. Gupta and M. Joshi. WSMP: Watson Sparse Matrix Package (2001). IBM Research Report RC22038 (98932).
[5] R. Fitzpatrick. Phys. Plasmas **2**, 825 (1995).
[6] Q. Yu. Phys. Plamas **13**, 062310 (2006).
[7] R. Carrera, R. D. Hazeltine, and M. Kotschenreuther. Phys. Fluids **29**, 899 (1986).
[8] C. C. Hegna and J. D. Callen. Phys. Fluids B **4**, 1855 (1992).
[9] H. Zohm, G. Gantenbein, A. Gude, S. Günter, *et al.*. Nucl. Fusion **41**, 197 (2001).
[10] M. Lehnen, S. Abdullaev, W. Biel, S. Brezinsek, *et al.*. J. Nucl. Mater. **337–339**, 171 (2005).
[11] T. Evans, R. Moyer, J. Watkins, P. Thomas, *et al.*. J. Nucl. Mater. **337–339**, 691 (2005).
[12] A. B. Rechester and M. N. Rosenbluth. Phys. Rev. Lett. **40**, 38 (1978).
[13] T. H. Stix. Nucl. Fusion **18**, 353 (1978).
[14] B. B. Kadomtsev and O. P. Pogutse. In: Plasma Physics and Controlled Nuclear Fusion Research, Proceedings of the 7th International Conference, volume 1, page 649. Innsbruck, Austria (1978).
[15] J. A. Krommes, C. Oberman, and R. G. Kleva. Journal of plasma physics **30**, 11 (1983).
[16] P. C. Liewer. Nuclear Fusion **25**, 543 (1985).
[17] M. Rover, A. M. R. Schilham, A. Montvai, and N. J. L. Cardozo. Phys. Plasmas **6**, 2443 (1999).